Basic Study on Gyroscopic Sensor using Active Magnetic Bearing

Yutaka MARUYAMA, Masaya TAKASAKI,Yuji ISHINO and Takeshi MIZUNO

Control Engineering Laboratory
Saitama University
Simo-Okubo 255, Sakuraku, Saitama, 338-8570, Japan
maruyama@mech.saitama-u.ac.jp

Takayuki ISHIGAMI and Hironori KAMENO

Research & Development Center
JTEKT CORPORATION
Toichi-cho. 333, Kashihara, Nara 634-8555, Japan
hironori_kameno@jtekt.co.jp

Abstract **– The paper proposes to apply a five degree-of-freedom active magnetic bearing (AMB) for developing compact, multi-axis, high-accuracy and low-cost gyroscopic sensors. In the proposed sensor, angular velocity and acceleration are measured based on the control signal for maintaining the relative position of the shaft to the stator in the AMB. It works as a two-axis gyroscopic sensor and also as a three-axis servo-type accelerometer so that the cost performance of the proposed sensor is expected to be high enough. In order to investigate its feasibility, several basic studies are carried out with a conventional-size AMB.**

Index Trem **– Gyroscopic sensor, Active magnetic bearing, Servo-type accelerometer, Angular velocity measurement, multi-axis sensor**

I. INTRODUCUTION

Gyroscopic sensor is used to measure angular velocity. There are a lot of applications such as navigation, homing and attitude control. In the fields of automobile, robot and micro unmanned air plane, compact and high-accuracy gyroscopic sensor are required to realize sophisticated motion and attitude control. Gyroscopic sensors are classified into various types according to the principle of operation. In low-cost applications, vibrating gyros are mostly used. However their detection sensitivity is low so that they are not suitable for high-performance applications.

We focus attention on rotating gyro because it has higher detection sensitivity than vibrating gyro, and propose to apply an AMB to rotating gyro in order to realize a compact, high-accuracy, multi-axis, and low-cost sensor. Even though AMB has been used for accelerometers or gyroscopic sensors in previous researches [1], [2], AMB has just supported a rotor or gimbals not directly been used to measure angular velocity. In contrast the proposed sensor works as a two-axis gyroscopic sensor and also as a three-axis servo-type accelerometer, which utilizes the control function of AMB. This paper will present the principle of angular velocity detection by the AMB. In order to examine the principle and investigate the feasibility of the proposed sensor, several basic studies are carried out with a conventional-size AMB.

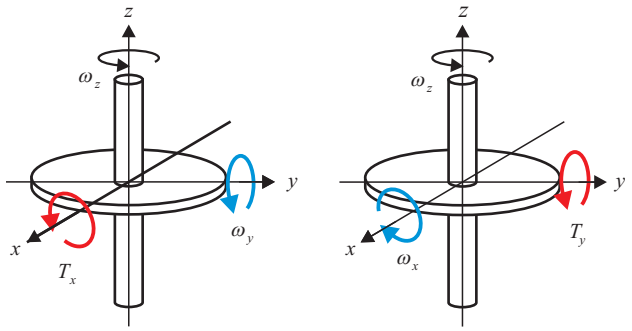

Fig. 1 Gyroscopic action.

II. ROTATING GYRO

A. Gyroscopic Action

Gyroscopic action is a motion that based on the law of angular momentum. When a rotor spins about the *z*-axis at a constant angular velocity, ω_z, the motion called precession arises about the *y*-axis if a torque acts about the *x*-axis in a right-hand coordinate system, as shown in Fig. 1. Pressesion about the *x*-axis also arises if a torque acts about the *y*-axis. This torque is presented as the product of angular momentum *H* and angular veloscity of precession, ω_x or ω_y. The equations of the torques are written as follows.

$$\begin{cases} T_x = H\omega_y , \\ T_y = -H\omega_x , \end{cases} \tag{1}$$

where

T_x, T_y : gyroscopic torque,
$H = I_z\omega_z$,
I_z : the moment of inertia about the *z*-axis.

B. Conventional Rotating Gyro

A rate-integrating gyro is shown in Fig. 2 [2] as an example of conventional rotating gyro. A flywheel is mounted in a gimbal, and the gimbal is supported by bearings. The flywheel spins at high rate. It has angular momentum, *H*. If the gyro itself rotates about the input axis, gyroscopic action rotates the flywheel with the gimbal about the output axis that is orthogonal to the spin axis and the input axis. A pickoff detects the relative angle of the

gimbal to the base. In order to cancel the deviation, the pickoff output drives a servo amplifier that supplies a current to the torque motor, commonly called torquer. Angular velocity can be measured based on the current because the control torque produced by the torquer cancel the precession torque and correlate with the current. The detection sensitivity of a rotating gyro is become high if the spin rate of the flywheel is high. Therefore, a rotating gyro is superior to other gyros in terms of detection sensitivity. However, friction in the bearings that support gimbal and flywheel generates drag torque. The friction also causes a drift in the output. Therefore sometimes the special bearings are used in the gyro or the flywheel is soused in the special liquid or gas to solve the problem as in [2].

C. *Magnetic Levitation Gyro*

In this study, a five-degree-of-freedom active magnetic bearing as shown in Fig. 3 is applied to gyroscopic sensor. We refer to the gyroscopic sensor as magnetic levitation gyro. Ten electromagnets and five displacement sensors is used in the AMB. Two electromagnets (***9***, ***10***) control the axial translation. The other electromagnets (***1*** - ***8***) control the radial translations and rotations. These electromagnets and sensors control the five-axis motions independently.

If the stator of AMB is moved, the relative displacement of the shaft of AMB to the stator changes due to the inertia of the shaft. The control system works to return the relative displacement to the original one. The force required for the recovery can be estimated from the control signal. Therefore, AMB has a function of servo-type accelerometer. In addition, if the shaft spins, precession torque appears and the torque can be estimated from the control signal. The angular velocity can be determined according to (1). Therefore it is possible to measure the five-axis motions of the measuring object on which the AMB is mounted.

In the proposed gyro there is not problem due to friction since the shaft is supported by magnetic forces. The gyro does not need any gimbal because the support mechanism works like two-axis gimbal. The gyro can measure five-axis motions. Therefore, high-accuracy, compact and low-cost sensor can be realized.

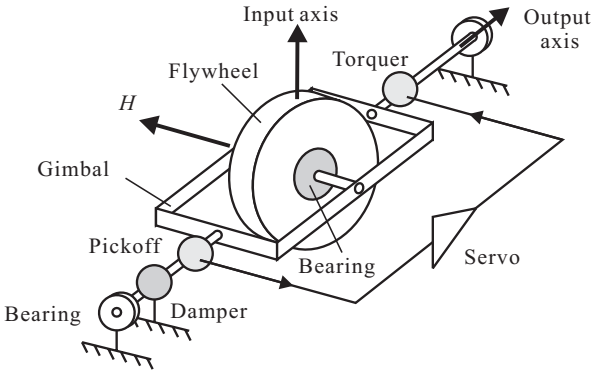

Fig. 2 Schematic view of a rate integrating gyro.

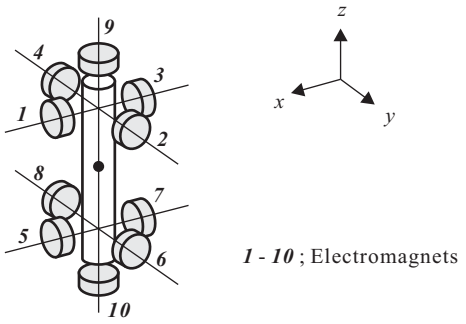

Fig. 3 Five-degree-of-freedom (5 DOF) active magnetic bearing.

III. Detecting Two-Axis Angular Velocities

There is mutual interference between two-axis rotations because of gyroscopic action. The mutual interference is a problem measuring angular velocities. The control signal includes components counterbalancing both gyroscopic torque coming from angular velocity about *x*-axis and inertial torque coming from angular acceleration about *y*-axis. Therefore the special signal processing is necessary when AMB measures two-axis angular velocities. The principle of detecting two-axis angular velocities is presented in this chapter. A model of rotational motions in an AMB is shown in Fig. 4. The angle θ is the angle of the shaft of AMB, φ is the angle of the stator of AMB, and ϕ is the relative angle of the shaft to the stator. Subscripts, *x* and *y* indicate the motions about each axis. thus,

$$\phi_x = \theta_x - \varphi_x, \quad \phi_y = \theta_y - \varphi_y. \tag{2}$$

When the stator rotates about *x* and *y*-axis, control torques T_{cx} and T_{cy} produced by the electromagnets, inertial torques and gyroscopic torques act on the shaft as shown in Fig. 4. Assuming that the shaft is axially symmetric, torque balance equations are written as follows.

$$\begin{cases} -I_r\ddot{\theta}_x - I_z\omega_z\dot{\theta}_y + T_{cx} = 0, \\ -I_r\ddot{\theta}_y + I_z\omega_z\dot{\theta}_x + T_{cy} = 0, \end{cases} \tag{3}$$

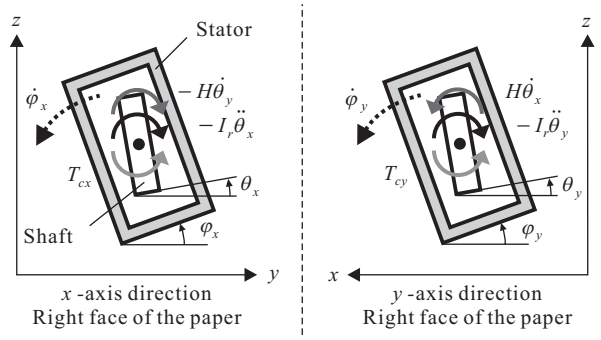

Fig. 4 A model of rotational motions in a 5 DOF active magnetic bearing.

where

I_r : principal moment of inertia of the shaft

Equation (3) is presented by

$$\begin{cases} \ddot{\theta}_x + a_k \dot{\theta}_y = T_{cx} / I_r , \\ \ddot{\theta}_y - a_k \dot{\theta}_x = T_{cy} / I_r . \end{cases} \tag{4}$$

where

$$a_k = I_z \omega_z / I_r . \tag{5}$$

Adding $\begin{cases} -\ddot{\varphi}_x - a_k \dot{\varphi}_y \\ -\ddot{\varphi}_y + a_k \dot{\varphi}_x \end{cases}$ to both side of (4) gives the solution:

$$\begin{cases} \ddot{\phi}_x + a_k \dot{\phi}_y = -\ddot{\varphi}_x - a_k \dot{\varphi}_y + T_{cx} / I_r , \\ \ddot{\phi}_y - a_k \dot{\phi}_x = -\ddot{\varphi}_y + a_k \dot{\varphi}_x + T_{cx} / I_r . \end{cases} \tag{6}$$

It is assuming that all the electromagnets are same and located at the distance of l from the center of gravity of the shaft. As in [3], the control torque is given by

$$\begin{aligned} T_{cx} &= K_i l u_{\theta x} + 4 K_d l^2 \phi_x , \\ T_{cy} &= K_i l u_{\theta y} + 4 K_d l^2 \phi_y , \end{aligned} \tag{7}$$

where

u_θ : control signal

ϕ : relative angle of the shaft to the stator

K_i and K_d are the values determined from the characteristics of the electromagnet, bias-current and the gap between the electromagnet and the shaft at steady state. Substituting (7) into (6), gives

$$\begin{cases} \ddot{\phi}_x + a_k \dot{\phi}_y - K_s \phi_x = b_\theta u_{\theta x} - \ddot{\varphi}_x - a_k \dot{\varphi}_y , \\ \ddot{\phi}_y - a_k \dot{\phi}_x - K_s \phi_y = b_\theta u_{\theta y} - \ddot{\varphi}_y + a_k \dot{\varphi}_x , \end{cases} \tag{8}$$

where

$$b_\theta = K_i l / I_r , \tag{9}$$

$$K_s = 4 K_d l^2 / I_r . \tag{10}$$

If the shaft is not displaced relatively from the stator by active control, the left-hand side of (8) is zero. Then (8) becomes

$$b_\theta \begin{bmatrix} u_{\theta x} \\ u_{\theta y} \end{bmatrix} - \begin{bmatrix} 1 & 0 \\ 0 & 1 \end{bmatrix} \begin{bmatrix} \ddot{\varphi}_x \\ \ddot{\varphi}_y \end{bmatrix} - \begin{bmatrix} 0 & a_k \\ -a_k & 0 \end{bmatrix} \begin{bmatrix} \dot{\varphi}_x \\ \dot{\varphi}_y \end{bmatrix} = 0 , \tag{11}$$

$$\therefore \quad b_\theta \begin{bmatrix} u_{\theta x} \\ u_{\theta y} \end{bmatrix} = \begin{bmatrix} s & a_k \\ -a_k & s \end{bmatrix} \begin{bmatrix} \dot{\varphi}_x \\ \dot{\varphi}_y \end{bmatrix} . \tag{12}$$

From (12), we get

$$\begin{bmatrix} u_{\theta x} \\ u_{\theta y} \end{bmatrix} = \frac{1}{b_\theta} \begin{bmatrix} s & a_k \\ -a_k & s \end{bmatrix} \begin{bmatrix} \dot{\varphi}_x \\ \dot{\varphi}_y \end{bmatrix} . \tag{13}$$

The solution to (13) is given by

$$\begin{bmatrix} \dot{\varphi}_x \\ \dot{\varphi}_y \end{bmatrix} = \frac{b_\theta}{s^2 + a_k^{\,2}} \begin{bmatrix} s & -a_k \\ a_k & s \end{bmatrix} \begin{bmatrix} u_{\theta x} \\ u_{\theta y} \end{bmatrix} . \tag{14}$$

Therefore, The two-axis (x-axis and y-axis) angular velocities can be estimated from the control signals for two-axis rotations.

IV. Experiment

A. Experimental Appratus and Methods

In order to verify the principle of detecting two-axis angular velocities as explained in the previous chapter, several experiments were caried out with a conventinal-size AMB system. The mesurements of single-axis angular velocity were carried out as a first step of verifying the principle of detecting two-axis angular velocities. The developed experimental apparatus is shown in Fig. 5. The AMB and a high-accuracy fiber optical gyro for reference (FOG) were put on a turntable. The turntable was driven by a servo motor to swing. In this case, the x-axis is the input axis of the AMB. The input axis of the AMB and the FOG is pointed to the vertical direction. The rotaitional axis of turntable is also pointed to the vertical direction. Therefore the turntable generated same angular velocities to the AMB and the FOG. The angular velocities measured by the AMB and the FOG were compared.

The turntable generates angular velocity about the x-axis only to the AMB in this setup. Considering this condition,

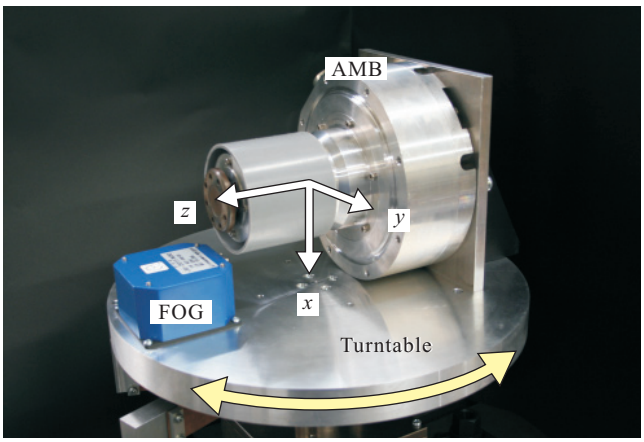

Fig. 5 Experimental apparatus.

$\dot{\varphi}_y$ equals zero in (13). Therefore the estimated equation is represented as

$$\dot{\varphi}_x = -\frac{b_\theta}{a_k} u_{\theta y} . \tag{15}$$

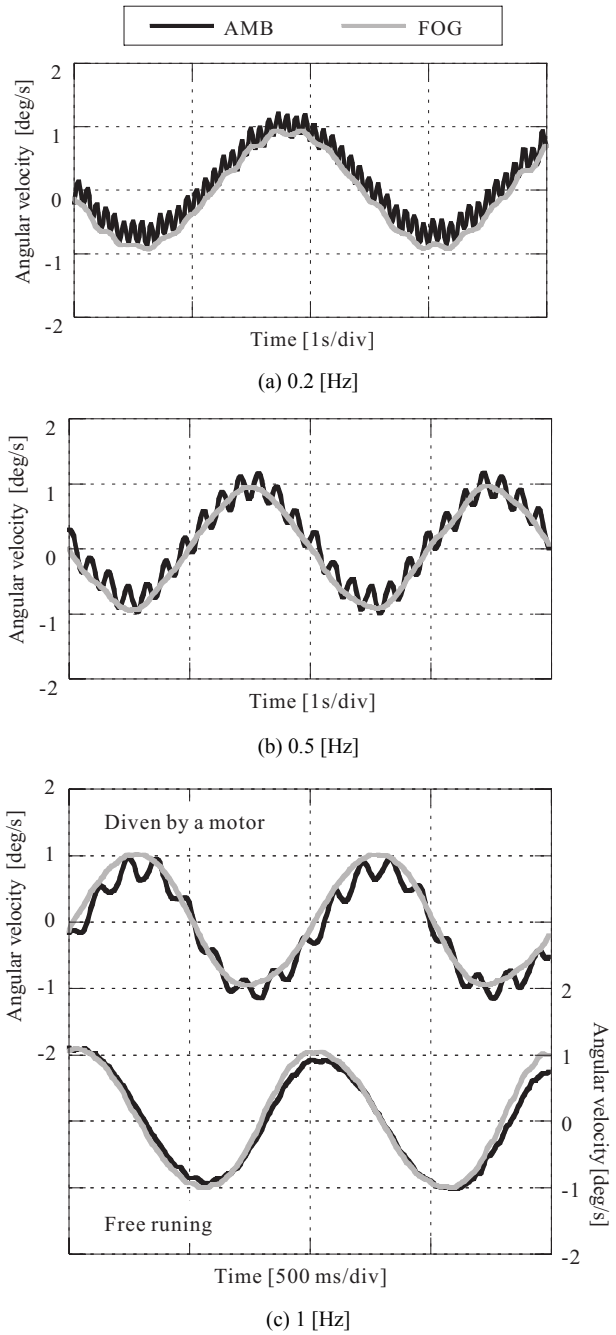

Fig. 6 Measurement of angular velocity about the *x*-axis.

Equation (15) was used to estimate the angular velocity in the following measurements.The mass of the shaft is 0.87 kg. The shaft of AMB was driven by a induction motor. The spining rate was 155 rps. The AMB is cotrolled by I-PD controllers independently in the five-axis (*x*, *y*, *z*-axis translations and *x*, *y*-axis rotations).

B. Experimental Results

The experimental results are shown in Fig. 6. The results show the angular velocity when the turntable was driven to oscillate sinusoidally at (a) 0.2, (b) 0.5 and (c) 1 Hz, respectively. The angular velocity estimated from the control currents of AMB agrees well with the output of FOG. There is a minor difference between the phase of the AMB output and the phase of the FOG output. The error of the amplitude is approximately 2 %. Such a error can be eliminated by proper calibration. Therefore, these results demonstrate that the AMB can mesure a single axis angular velocity. However it is found that the estimated signal includes a component of approximately 8 Hz. This component appears when the motor drives the shaft and disappears when the shaft runs freely. Therefore, it may be caused by the motor drive. Motor drive should be considered in designing a gyroscopic sensor.

V. CONCLUSION

Gyroscopic sensor using AMB was proposed. The principle of detecting two-axis angular velocities in the proposed sensor was derived based on the dynamics of the AMB. Several experiments were carried out to examine the principle. The results showed that the AMB could measure single-axis angular velocity. Two-axis angular velocity measurements will be carried out as a next step. In future, we will miniaturize the AMB and try to optimize it in the way of using gyro sensor. We will investigate about a controller and method of signal processing because the accuracy of the proposed sensor depends on their performance.

REFERENCES

[1] M. Takizawa, M. Otsuki, T. Suzuki, “Study of A Floated Pendulum Accelerometer with Passive Magnetic Suspension,” Technical Report of National Aerospace Laboratory, TR-644, December, 1980 (In Japanese)

[2] A. Lawrence, “Modern inertial technology: navigation, guidance, and control”, Springer-Verlag, 1992.

[3] T. Miizuno, T. Higuch, “Design of The Control System of Totally Active Magnetic Bearings – Structures of The Optimal Regulator –,” International Symposium on Design and Synthesis, Tokyo Japan, pp.534-539, July 11-13, 1984